Supplementary Information

L-cysteine capped MoS2 QDs for dual-channel imaging and superior Fe3+ ion sensing in biological systems

*Vishakha Takhar[1], Simranjit Singh[2], Superb K Misra[2], Rupak Banerjee[1,3]**

[1]Department of Physics, Indian Institute of Technology Gandhinagar, Palaj, Gandhinagar 382355, India

[2]Materials Engineering, Indian Institute of Technology Gandhinagar, Palaj, Gandhinagar 382355, India

[3]K C Patel Centre for Sustainable Development, Indian Institute of Technology Gandhinagar, Palaj, Gandhinagar 382355, Gujarat, India

**Corresponding author: rupakb@iitgn.ac.in*

Supplementary Figures:

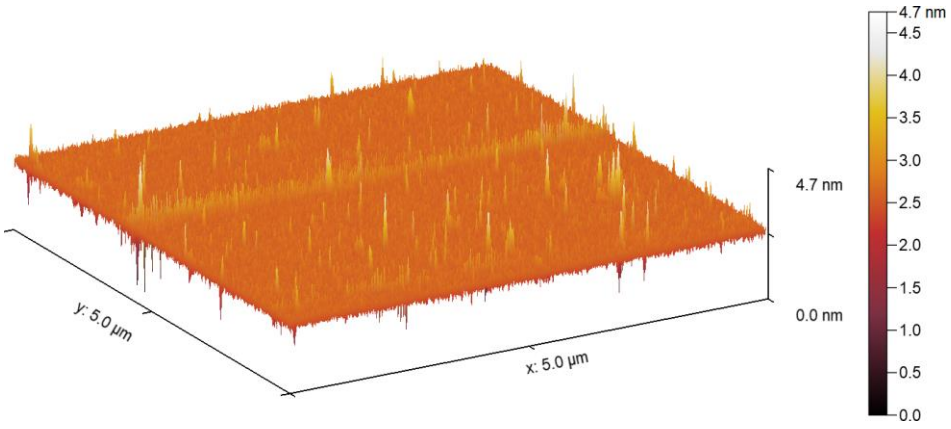

Figure S1: 3D AFM image of MQDs revealing their height profile.

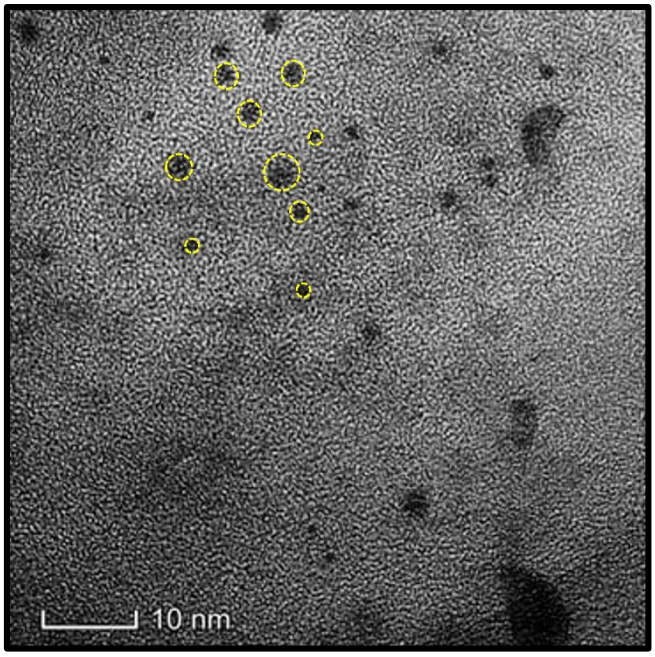

Figure S2: a) High magnification TEM images of MQDs used for calculation of size distribution.

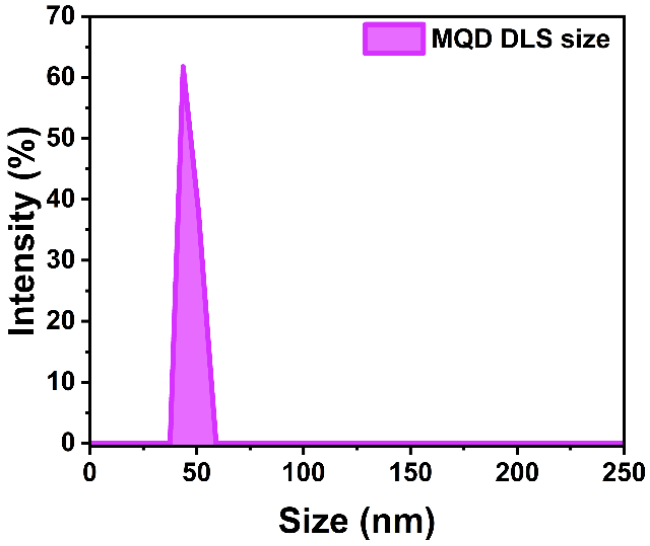

Figure S3: Dynamic light scattering based hydrodynamic size of MQDs.

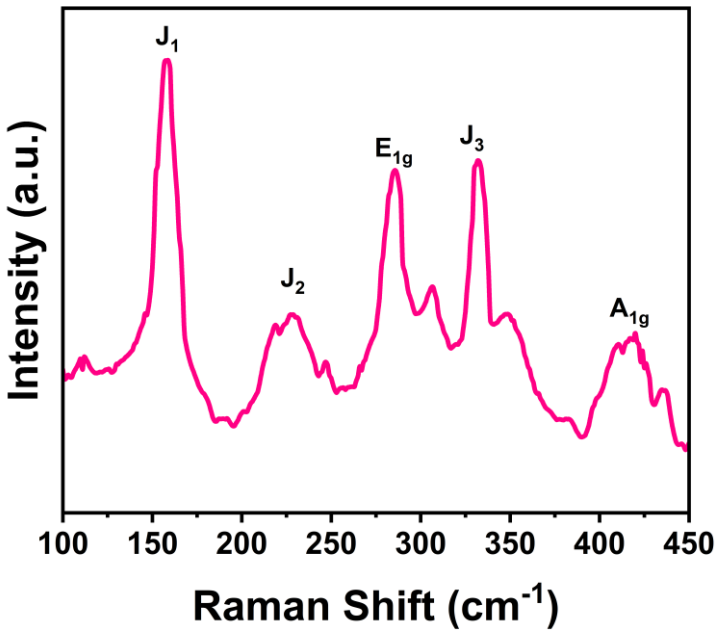

Figure S4: Raman spectra of synthesized MoS_2 quantum dots showing 1T phase of MQDs.

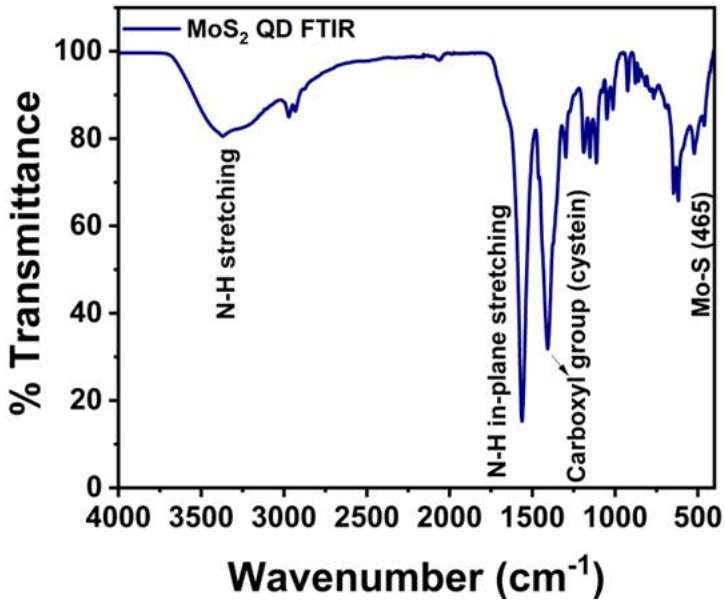

Figure S5: FTIR spectra of synthesized MQDs

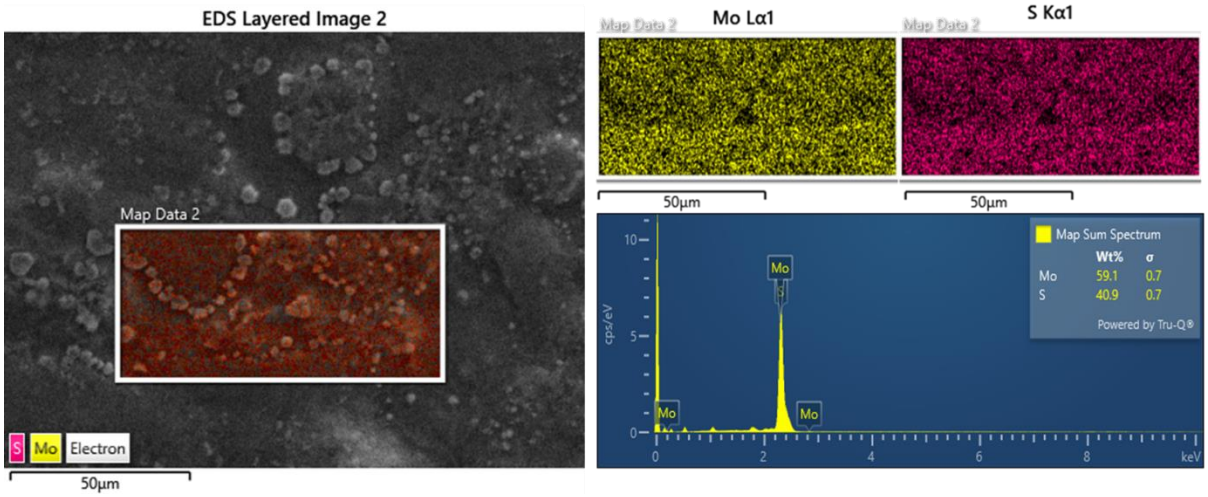

Figure S6: FESEM image with EDS mapping of MQDs.

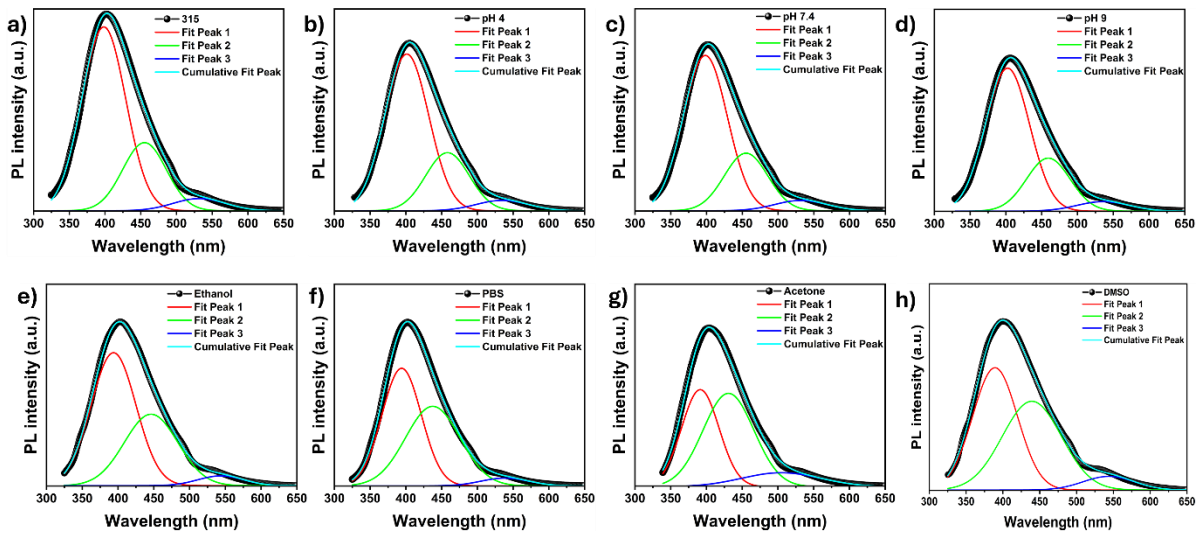

Figure S7: The fitted PL profiles of MQDs in a) Ultrapure water, b) at pH 4, c) at pH 7.4, d) at pH 9, e) in ethanol, f) in PBS, g) in Acetone, and h) DMSO media under 315 nm excitation.

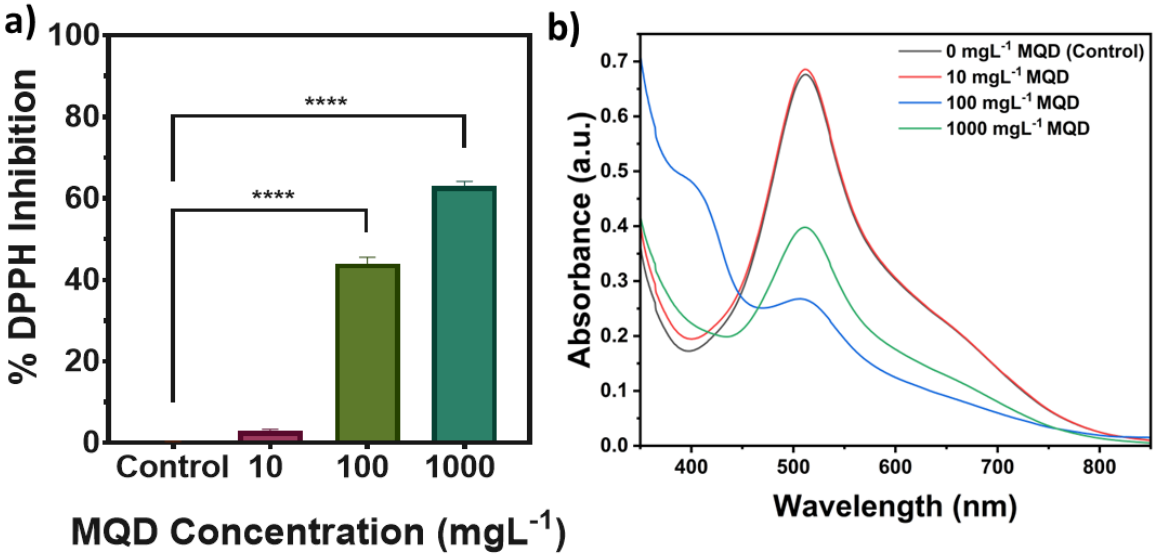

Figure S8: Concentration-based DPPH scavenging efficiency a) comparative bar plots and b) respective UV-Vis plots with 0 - 1000 mg L^{-1} of MQDs representing its antioxidant properties.

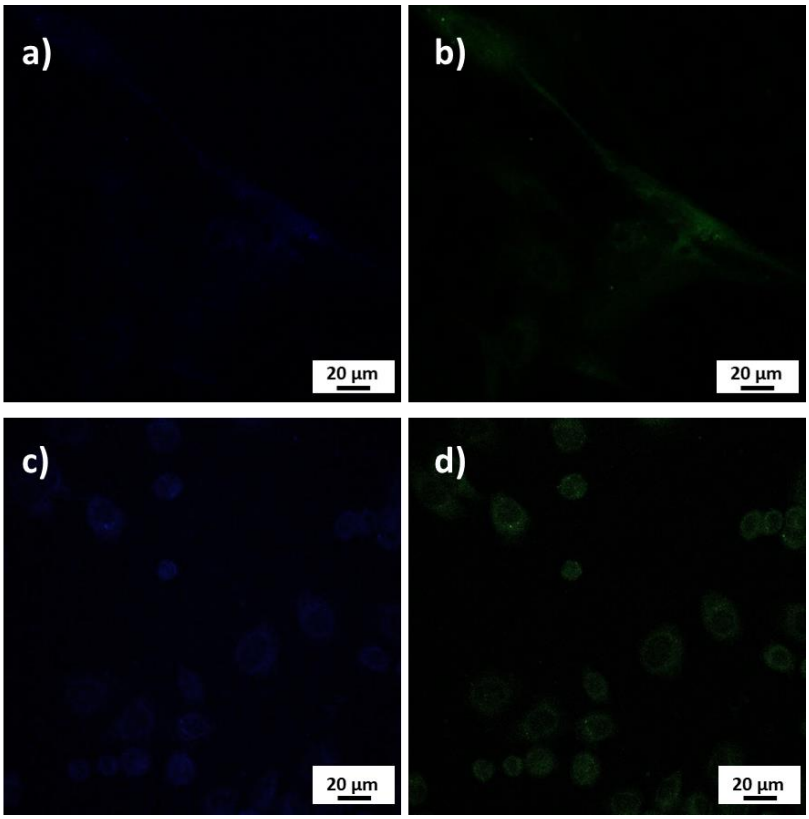

Figure S9: Autofluorescence images of a) RPE-1 cell line in the blue channel, b) RPE-1 cell line in the green channel, c) SK-BR-3 cell line in the blue channel d) SK-BR-3 cell line in the green channel.

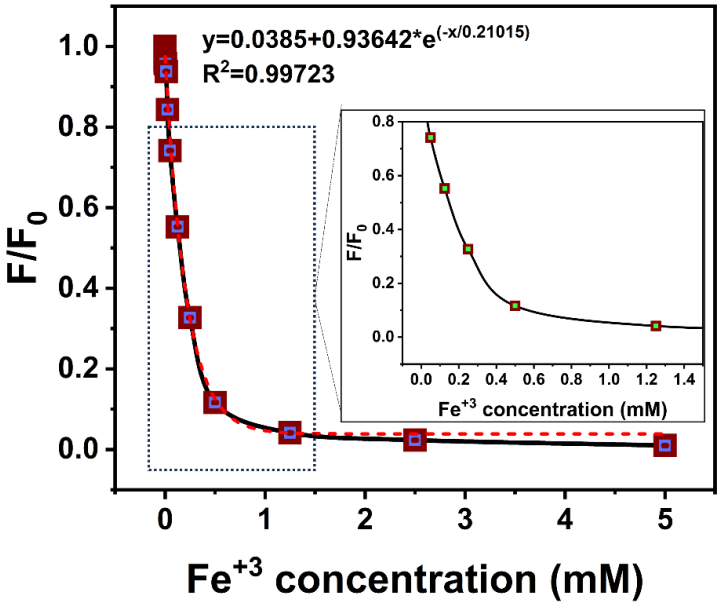

Figure S10: Fitting of the fluorescence intensity versus Fe^{3+} concentration from 0 to 5 mmol.

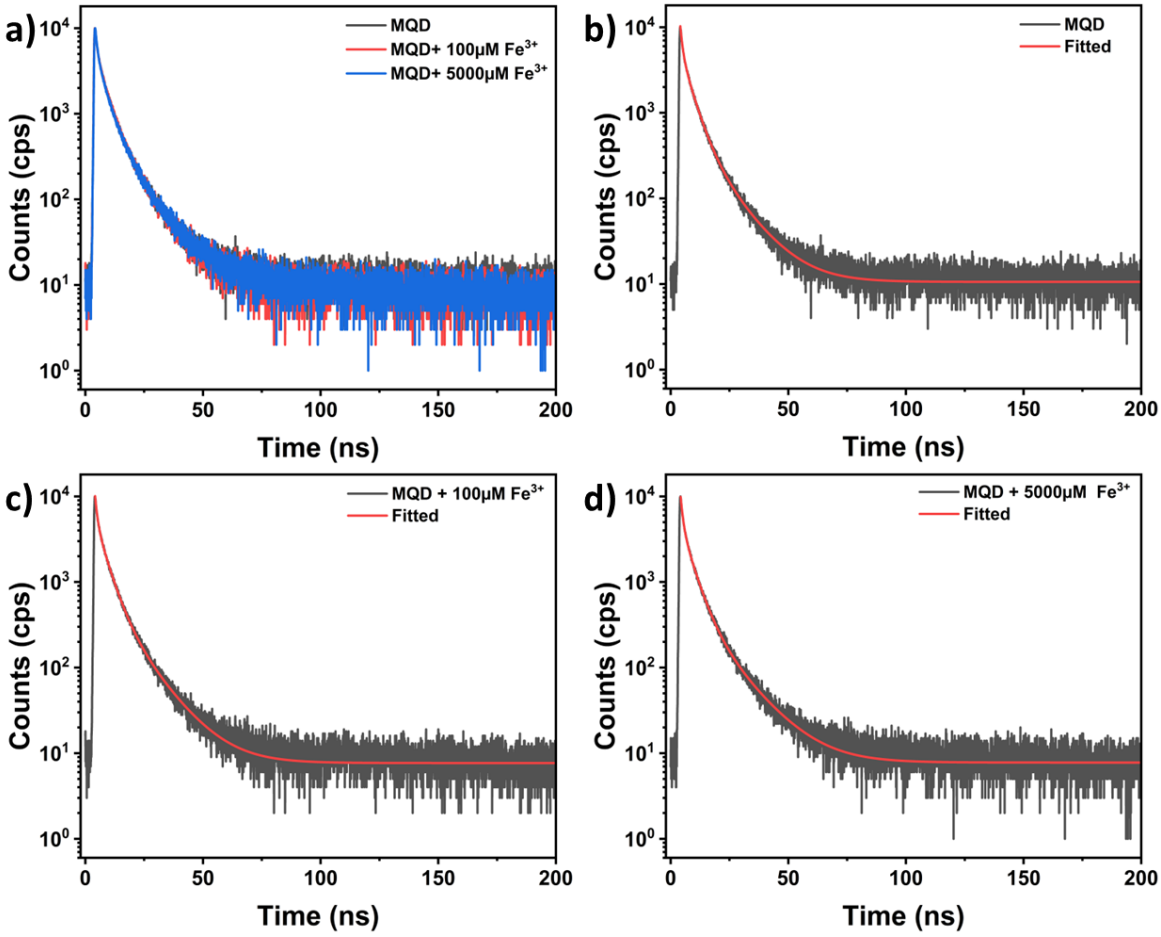

Figure S11: a) Comparative time-resolved photoluminescence of MQDs, MQDs with 100 µM and 5000 µM of Fe^{3+} ions. The respective fitting plots are shown for b) pristine MQDs, c) MQDs with 100 µM of Fe^{3+} ions, and d) MQDs with 5000 µM of Fe^{3+} ions.

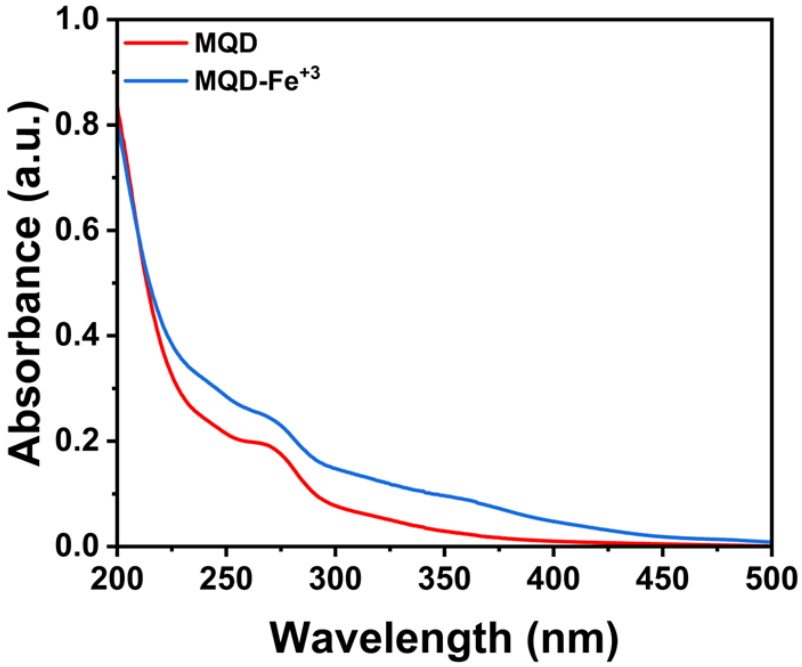

Figure S12: Comparative UV-Vis spectra of MQDs before and after the addition of Fe^{3+} ions.

Supplementary Tables:

Table S1: The fitted peak positions of MQDs under various conditions.

Suspension System (excitation at 315nm)	**Peak 1 (nm)**	**Peak 2 (nm)**	**Peak 3 (nm)**
pH 4	401.28 ± 0.59	458.22 ± 1.24	534.75 ± 4.28
pH 7.5 (Ultrapure Water)	398.27 ± 0.58	455.21 ± 1.25	531.83 ± 4.22
pH 9	402.28 ± 0.56	455.21 ± 1.27	535.81 ± 4.24
PBS	394.07 ± 0.67	437.57 ± 0.5.19	538.46 ± 3.67
Ethanol	393.71 ± 1.26	446.18 ± 4.46	534.44 ± 3.87
Acetone	391.35 ± 1.46	430.80 ± 7.51	504.52 ± 21.17
DMSO	389.29 ± 1.60	439.32 ± 7.67	543.70 ± 4.97

Table S2: Chemical composition of simulated body fluid (SBF) solution

S. No.	Reagents Used	Grams in 1000mL
1.	NaCl	8.035
2.	$NaHCO_3$	0.355
3.	KCl	0.225
4.	$K_2HPO_4.3H_2O$	0.231
5.	$MgCl_2.H_2O$	0.311
6.	1M HCl	40mL
7.	$CaCl_2$	0.292
8.	Na_2SO_4	0.072
9.	$((CH_2OH)_3CNH_2)$	6.118
10.	1M HCl	Appropriate amount for adjusting the pH 7.4

Table S3: Analytical results of Fe^{+3} recovery in biological samples

Samples	Added Fe^{+3} (µM)	Measured (µM)	Recovery (%)
PBS	0.25	0.246	97.2 ± 1.43
	1	1.019	101.9 ± 2.26
	5	4.89	97.8 ± 2.42
SBF	0.25	0256	102.4 ± 2.96
	1	0.983	98.3 ± 2.53
	5	5.08	101.6 ± 2.03

Table S4: Comparative decay time analysis of MQDs, MQDs with 100 μM and 5000 μM of Fe^{3+}ions.

Sample	**τ_1 (ns)**	**τ_2 (ns)**	**τ_3 (ns)**	**τ_{av}**	**Ratio**
MQD	0.859 ± 0.017	4.042 ± 0.048	11.515 ± 0.149	5.575 ± 0.089	1
MQD+ 100μM Fe^{3+}	0.848 ± 0.017	4.111 ± 0.047	11.644 ± 0.142	5.69 ± 50.085	0.98
MQD+ 5000μM Fe^{3+}	0.905 ± 0.016	4.233 ± 0.047	12.821 ± 0.159	5.843 ± 0.090	0.95

Table S5: Comparative binding energies of Mo and S before and after Fe^{+3} detection using MQDs

SnO.	**Sample**	**Binding Energy**	
		Mo	**S**
1.	MQD	229.4	163.4
2.	MQD with Fe^{3+}	229.4	163.4